Theoretical Study of the Gas-Phase Chemiionization Reactions La + O and La + O_2

Tanya K. Todorova, Ivan Infante, and Laura Gagliardi*

Department of Physical Chemistry, University of Geneva, 30 Quai Ernest Ansermet, CH-1211 Geneva, Switzerland

John M. Dyke*

Department of Chemistry, University of Southampton, Highfield, Southampton SO17 1BJ, United Kingdom

Received: May 23, 2008; Revised Manuscript Received: June 19, 2008

The La + O and La + O_2 chemiionization reactions have been investigated with quantum chemical methods. For La + $O_2(X^3\Sigma_g)$ and La + $O_2(a^1\Delta_g)$, the chemiionization reaction La + $O_2 \rightarrow LaO_2^+ + e^-$ has been shown to be endothermic and does not contribute to the experimental chemielectron spectra. For the La + $O_2(X^3\Sigma_g)$ reaction conditions, chemielectrons are produced by La + $O_2 \rightarrow$ LaO + O, followed by La + O → $LaO^+ + e^-$. This is supported by the same chemielectron band, arising from La + O → $LaO^+ + e^-$, being observed from both the La + $O(^3P)$ and La + $O_2(X^3\Sigma_g)$ reaction conditions. For La + $O_2(a^1\Delta_g)$, a chemielectron band with higher electron kinetic energy than that obtained from La + $O_2(X^3\Sigma_g)$ is observed. This is attributed to production of $O(^1D)$ from the reaction La + $O_2(a^1\Delta_g) \rightarrow$ LaO + $O(^1D)$, followed by chemiionization via the reaction La + $O(^1D) \rightarrow LaO^+ + e^-$. Potential energy curves are computed for a number of states of LaO, LaO* and LaO^+ to establish mechanisms for the observed La + O → $LaO^+ + e^-$ chemiionization reactions.

1. Introduction

Chemiionization reactions are an interesting class of gas-phase reactions that can occur between ground state reagents.[1–3] They play important roles, for example, in the earth's upper atmosphere, in flames and in magnetohydrodynamic plasmas. Chemielectron spectroscopy has been defined as the study of the energy and intensity distribution of electrons that are produced as a result of a chemiionization reaction,[4] which in turn has been defined[5] as a reaction in which the number of charge carriers is increased as a direct result of the formation of new chemical bonds. These reactions have been found to occur in the gas phase between a metal with unfilled d or f shells, and a number of oxidants, and mass spectra of the ions produced and associated electron energy distributions have been recorded for a number of metal−oxidant reactions. Relevant to the present work is a systematic experimental study that has been performed of some gas-phase lanthanide (Ln) plus oxidant ($O_2(X^3\Sigma_g)$, $O_2(a^1\Delta_g)$ or $O(^3P)$) reactions using chemielectron spectroscopy.[4,6,7] In these studies, an effusive beam of the selected lanthanide is crossed with an effusive beam from (A) a microwave discharge of flowing oxygen which contains $O_2(X^3\Sigma_g)$, $O_2(a^1\Delta_g)$ or $O(^3P)$, (B) the above microwave discharge conditions but with $O(^3P)$ deactivated, or (C) pure $O_2(X^3\Sigma_g)$. By comparing the chemielectron spectra and the mass spectra obtained from these three reactions conditions, the chemielectron spectra were attributed to the following chemiionization reactions

$$Ln + O(^3P) \rightarrow LnO^+ + e^-$$
$$Ln + O_2(X^3\Sigma_g) \rightarrow LnO_2^+ + e^-$$
$$Ln + O_2(a^1\Delta_g) \rightarrow LnO_2^+ + e^-$$

In the original experimental work,[6,7] because the experiments were carried out under effusive flow conditions, it was recognized that secondary reactions may well be contributing to the observed chemielectron spectra, and it was found valuable to estimate the standard enthalpy of the eleven reactions, shown in Table 1 for lanthanum, to provide supporting thermodynamic information that could help to identify the major secondary reactions. For example, for the lanthanide metal, Ln, the Ln + $O_2 \rightarrow$ LnO + O reaction may be rapid (reaction 5 in Table 1) and this could provide O atoms for the secondary, chemiionization reaction Ln + O → $LnO^+ + e^-$ (reaction 6 in Table 1). Reaction 5 followed by reaction 6 has already been demonstrated as the source of the chemielectron band observed in a study of the U + O_2 chemiionization reaction.[8,9]

In the experimental study of lanthanum with the oxidants $O_2(X^3\Sigma_g)$, $O_2(a^1\Delta_g)$ and $O(^3P)$,[6,7] the La + $O_2(X^3\Sigma_g)$ reaction gave a chemielectron band with a most probable kinetic energy (MPKE) (band maximum) of 1.03 ± 0.20 eV and a high kinetic energy offset (HKEO) of 1.5 ± 0.1 eV. For the La + $O_2(a^1\Delta_g)$ reaction, these values were 2.41 ± 0.06 and 3.3 ± 0.1 eV, whereas for the La + $O(^3P)$ reaction they were 0.67 ± 0.06 and 1.8 ± 0.1 eV. Unfortunately, experimentally available thermodynamic values for LaO, LaO^+, LaO_2 and LaO_2^+ are not sufficiently well determined to allow these values to be tested for the reactions proposed. However, it is now possible to investigate reactions of this type by quantum chemical methods which have been developed to treat heavy metal containing systems such as lanthanide or actinide oxides. Recently, two metal plus oxidant chemiionization reactions, namely, Sm + O → $SmO^+ + e^-$ and U + O → $UO^+ + e^-$ were investigated computationally to establish the mechanism of chemiionization in terms of the states involved by comparing theoretical and experimental chemielectron band positions.[9,10] It is proposed to use these computational methods to investigate the chemiionization reactions which occur under the La + $O_2(X^3\Sigma_g)$, La + $O_2(a^1\Delta_g)$, and La + $O(^3P)$ reaction conditions.

The objective of this work, therefore, is to compute selected spectroscopic constants for LaO, LaO^+, LaO_2 and LaO_2^+, to make a comparison with available experimental values, and to

* Authors to whom correspondence should be addressed. E-mail: L.G., laura.gagliardi@chiphy.unige.ch; J.M.D., jmdyke@soton.ac.uk.

10.1021/jp804578d CCC: $40.75
Published on Web 08/01/2008

TABLE 1: Experimental and Computed Reaction Enthalpies (eV) for Possible Reactions (See Text)

reaction	reaction enthalpy from ref 6	computed values wrt $O_2(X^3\Sigma_g)$	computed values wrt $O_2(a^1\Delta_g)$
1. $La + O_2 \rightarrow LaO_2^+ + e^-$	-1.1 ± 1.5	1.51	0.55
2. $La + O_2 \rightarrow LaO^+ + O^-$	0.4 ± 1.2	1.38	0.42
3. $La + O_2 \rightarrow LaO^+ + O + e^-$	1.9 ± 1.2	2.78	1.82
4. $La + O_2 \rightarrow La^+ + O_2^-$	5.2 ± 0.1	5.20	4.24
5. $La + O_2 \rightarrow LaO + O$	-3.1 ± 0.1	−2.41	−3.37
6. $La + O \rightarrow LaO^+ + e^-$	-3.2 ± 0.3	−2.48	
7. $LaO^+ + O_2 \rightarrow LaO_2^+ + O$	2.1 ± 1.8	4.00	3.04
8. $LaO_2^+ + La \rightarrow LaO^+ + LaO$	-5.2 ± 1.9	−6.41	
9. $LaO_2^+ + M \rightarrow LaO^+ + O + M$	3.0 ± 1.8	1.26	
10.$LaO + O \rightarrow LaO_2^+ + e^-$	2.0 ± 0.9	3.93	
11.$LaO^+ + O + M \rightarrow LaO_2^+ + M$		−1.26	

Note that the first four reactions 1−4 are primary ionization reactions, whereas reactions 5−11 are neutral or ion−molecule processes. The separation of the reactions in this way follows the approach used in the previous experimental papers (refs 6 and 7).

compute the standard reaction enthalpies for the eleven reactions listed in Table 1. Also, by computing relevant parts of potential energy curves for LaO, LaO^+, LaO_2 and LaO_2^+, it was hoped that a mechanism for the La + O and La + O_2 chemiionization reactions investigated experimentally could be proposed.

2. Computational Details

This study on LaO LaO^+, and LaO_2 LaO_2^+ was performed using the complete active space (CAS) SCF method[11] followed by multiconfigurational second-order perturbation theory (CASPT2),[12] coupled cluster method with single, double and perturbative triple excitations, CCSD(T), and density functional theory (DFT). Scalar relativistic effects were included using the Douglas−Kroll Hamiltonian[13,14] and the relativistic ANO-RCC basis set,[15] where the primitive set of 24s21p15d5f3g functions was contracted to 11s10p8d5f3g for lanthanum and the primitive set of 14s9p4d3f2g basis functions was contracted to 8s7p4d3f for oxygen. In the CASSCF calculations, an active space of 7 electrons in 12 orbitals was used for LaO and an active space of 11 electrons in 12 orbitals was used for LaO_2. These orbitals are formed by linear combinations of 6s and 5d orbitals of La with 2p orbitals of O. For LaO, the 3p orbitals of O were also included in the CAS. In the subsequent CASPT2 calculations, [Xe] 4d orbitals of La and 1s orbitals of O were kept frozen. Spin−orbit coupling effects were computed by using the CASSCF state interaction (CASSI) method.[16,17] The approach has proven to be successful in the study of similar compounds containing heavy elements.[18–26] The CCSD(T) calculations employed the same active spaces as those in the perturbative part of the corresponding CASPT2 calculations. In total, 17 electrons were correlated for LaO, and 23 electrons were correlated for LaO_2. The DFT calculations were performed with the hybrid B3LYP functional[27] using the same basis sets for La and O. The calculations on LaO and LaO^+ were carried out imposing C_2 symmetry along the internuclear axis, whereas C_{2v} symmetry was employed for LaO_2 and LaO_2^+. Full geometry optimizations at the CASPT2, CCSD(T) and DFT levels of theory were followed by vibrational frequency calculations. The potential energy curves for several electronic states of LaO and LaO^+ were calculated at the CASPT2 level of theory. All the calculations were performed using the MOLCAS 7.0 program package.[28]

3. Results and Discussion

LaO and LaO^+. The ground state electronic configurations of La, La^+, and O atoms are [Xe] $5d^16s^2$, $^2D_{3/2}$, [Xe] $5d^2$, $^3F_2$, and [He] $2s^22p^4$, $^3P_2$, respectively. The ground states of LaO and LaO^+ are known to be $^2\Sigma^+$ and $^1\Sigma^+$, respectively from available experimental and theoretical evidence.[29,30] The computed equilibrium spectroscopic constants (equilibrium bond distance R_e, dissociation energy D_e, and harmonic vibrational constant ω_e) for the ground states of LaO and LaO^+ are presented in Table 2, along with the computed first ionization energies of La and LaO. Table 2 also summarizes results of previous theoretical studies on LaO and LaO^+. The calculated CASPT2 value of R_e for LaO is longer (by ca. 0.03 Å) than the experimental value, whereas the computed CASPT2 vibrational constant is in a very good agreement with experiment. The CASPT2 equilibrium distance of LaO^+ is 1.815 Å and the computed vibrational constant ω_e of LaO^+ is 849 cm^{-1}; the experimental ω_e value is 838 cm^{-1}.[31] Including spin−orbit coupling has a minor effect on these values. The computed first IEs of La and LaO are within the experimental error bars,[32,33] whereas the dissociation energies of both LaO and LaO^+ are lower than the experimentally obtained values. Nevertheless, the experimental values show that IE(La) > IE(LaO) and D_0(LaO) < D_0(LaO^+). These trends are reproduced by our calculations. The CCSD(T) and DFT/B3LYP results on LaO and LaO^+ agree very well with the CASPT2 values. According to our spin-free calculations at the equilibrium bond distance, the ground state of LaO is a nondegenerate $^2\Sigma^+$ state. The spin−orbit calculation reveals that it is a pure $^2\Sigma_{0.5}$ state with $\Omega = 0.5$. Similarly, the ground state of LaO^+ is a $^1\Sigma_0^+$ state with $\Omega = 0$.

LaO_2 and LaO_2^+. Experimental information on the geometrical structures of both LaO_2 and LaO_2^+ are not available. The optimized geometries for LaO_2 and LaO_2^+, their computed bond dissociation energies with respect to La + O_2 and La^+ + O_2, respectively, and the computed ionization energy of LaO_2 are given in Table 3. Neutral LaO_2 has a bent C_{2v} structure with a lanthanum−oxygen bond length of 1.979 Å and bond angle θ(O−La−O) of 136° (CASPT2 value). The R_e(La−O) bonds are elongated with respect to the equilibrium bond distance in LaO (1.855 Å). Energetically, the optimized linear structure is only 0.2 eV less stable than the bent geometry. According to our calculations, LaO_2 has a $^2B_1$ electronic ground state with the unpaired electron in a molecular orbital composed of 2p O orbitals. The cationic LaO_2^+ species arises upon removal of that electron with concomitant relaxation of the O−La−O angle to 180° and shortening of the lanthanum−oxygen bond length to 1.909 Å. The ground state of LaO_2^+ is a $^1\Sigma_g^+$ state. A bent geometry is also obtained for neutral LaO_2 at the DFT/B3LYP level of theory, with a bond angle of 135° (compared to the CASPT2 value of 136°) and a lanthanum−oxygen bond

TABLE 2: Computed Spectroscopic Constants for the Ground States of LaO and LaO^+[a]

system	method	R_e	D_e	ω_e	IE
La	CASPT2				5.51
	CCSD(T)				5.57
	DFT/B3LYP				5.63
	ACPF				5.52[b]
	expt				5.58[c]
LaO	CASPT2	1.855	7.70	804	5.19
	CCSD(T)	1.862/1.841[d]/1.869[e]	7.84/8.13[d]/7.92[e]	797/807[d]/794[e]	5.28
	DFT/B3LYP	1.858/1.828[f]/1.827[b]	7.80/8.24[f]/8.32[b]	818/800[b]/824[b]	5.47/5.36[f]
	DFT	1.89 (F)/1.84 (C)[g]	7.60 (F)/8.77 (C)[g]	761 (F)/814 (C)[g]	
	PPCI	1.81[h]	8.02[h]	847[h]	
	expt	1.826[i]	8.29[j]	813[i]/797[k]	4.95 ± 0.19[l]
LaO^+	CASPT2	1.815	8.02	849	
	CCSD(T)	1.817	8.13/7.72[m]	856	
	DFT/B3LYP	1.814/1.779[f]	7.96	877/889[f]	
	MP2	1.861[m]			
	expt		8.82 ± 0.23/8.88[n]	838[k]	

[a] This work unless otherwise indicated. Equilibrium bond distances (R_e) in Å, dissociation energies (D_e) in eV, and harmonic vibrational constants (ω_e) in cm^{-1}. First Ionization Energy (IE) for La and LaO is in eV. Previous calculations along with available experimental data are also listed. [b] Reference 36. [c] Reference 32. [d] Reference 37. [e] Reference 38. [f] Reference 39. [g] Reference 40; F = relativistic full DF with correlation and exchange-gradient corrections; C = correlation correction. [h] Reference 41; PPCI = pseudopotential CI with variable 4f occupation. [i] Reference 29; gas-phase spectroscopic measurements. [j] Reference 42. [k] Reference 31; from measurements in an argon matrix. [l] Reference 33. [m] Reference 30. [n] Reference 43.

TABLE 3: Computed Spectroscopic Constants for the Ground States of LaO_2 and LaO_2^+[a]

				D_e			
system	method	R_e	∠(O−La−O)	$O_2(X^3\Sigma_g)$	$O_2(a^1\Delta_g)$	ω_e	IE
LaO_2 C_{2v}	CASPT2	1.979	136	6.47	7.43	133 (ν_2), 340 (ν_3), 628 (ν_1)	7.99
	CCSD(T)			6.71			8.08
	DFT/B3LYP	1.976	135	6.62		130 (ν_2), 342 (ν_3), 630 (ν_1)	8.70
	expt			7.26 ± 0.45[b]		570 (ν_1)[c]	8.21 ± 0.92[b]
							9.5 ± 1.5[d]
							9.5 ± 0.5[e]
							8.12[f]
LaO_2^+ linear	CASPT2	1.909	180	3.99	4.95	154 (ν_2), 553 (ν_1), 716 (ν_3)	
	CCSD(T)			4.20			
	DFT/B3LYP	1.860	180	3.55		184 (ν_2), 643 (ν_1), 754 (ν_3)	
	expt			4.63 ± 0.47[b]/5.73[f]		689 (ν_3)[c]	

[a] This work unless otherwise indicated. Equilibrium bond distances (R_e) in Å, angles in (deg), dissociation energies (D_e) and ionization energies (IE) in eV, and harmonic vibrational constants (ω_e) in cm^{-1}. The dissociation energies of LaO_2 and LaO_2^+ are given with respect to La + O_2 and La^+ + O_2, respectively. The available experimental data are also listed. [b] Derived from D_0(OLa−O) of (4.20 ± 0.33) eV from ref 34. [c] From the matrix isolation infrared work of ref 31 measurements in an argon matrix. [d] Reference 44. [e] Reference 6. [f] Reference 43.

length of 1.976 Å (compared to the CASPT2 value of 1.979 Å). Rather poor agreement is obtained for the LaO_2^+ molecule, for which the R_e(La−O) DFT bond length deviates by ca. 0.05 Å from the corresponding CASPT2 value (1.860 Å). The CASPT2 computed harmonic vibrational wavenumbers for LaO_2 are 133, 340 and 628 cm^{-1}. The 133 cm^{-1} value is the deformation mode (ν_2) and the latter two values correspond to the antisymmetric (ν_3) and symmetric stretching (ν_1) of the La−O bonds, respectively. For the linear LaO_2^+, the computed wavenumbers are 154 (ν_2), 553 (ν_1) and 716 cm^{-1} (ν_3). The DFT frequencies are in agreement with the CASPT2 frequencies. The adiabatic ionization energy of LaO_2 computed at the CASPT2 level of theory is 7.99 eV, in a very good agreement with the CCSD(T) value of 8.08 eV, whereas the DFT value is significantly higher (8.70 eV). They are all well within the quoted error of the experimentally reported IE(LaO_2) of 8.21 ± 0.92 eV (derived from values in ref 34). As far as the LaO_2 dissociation energy is concerned, the calculated CASPT2 D_e value with respect to $O_2(X^3\Sigma_g)$ is 6.47 eV. This agrees reasonably well with the experimental result of 7.26 ± 0.45 eV (derived from values in ref 34). The energy to dissociate LaO_2^+ into La^+ and O_2 species is calculated at the CASPT2 level as 3.99 eV (with respect to $O_2(X^3\Sigma_g)$), in agreement with the experimental value of 4.63 ± 0.47 eV, derived from values in ref 34.

A prerequisite for a metal-plus-oxidant chemiionization reaction to take place is that the dissociation energy of the neutral metal oxide is greater than its adiabatic ionization energy. Clearly, this is not the case for LaO_2, with $D_e(LaO_2)$ = 7.26 ± 0.45 eV and IE(LaO_2) = 8.21 ± 0.92 eV (experimental values; the corresponding computed CASPT2 values in this work are 6.47 and 7.99 eV, respectively), indicating that the chemiionization reaction La + $O_2 \rightarrow LaO_2^+ + e^-$ is endothermic. On the other hand, D_e(LaO) > IE(LaO) from both experiment and theory, indicating that the La + O → $LaO^+ + e^-$ reaction is exothermic (see Table 2). At the time of the original study of the La + O_2 and La + O reactions by chemielectron spectroscopy,[6,7] ref 34 had not been published and the available thermodynamic values at that time indicated that $D_e(LaO_2)$ > IE(LaO_2).[6] However, the theoretical results of this work and the experimental results of ref 34 clearly show that is not the case.

Interpretation of Experimental Chemielectron Spectra. The chemielectron spectra obtained under La + $O_2(X^3\Sigma_g)$ conditions gave a band maximum, MPKE value, of 1.03 ± 0.20

eV and a high kinetic energy offset of 1.5 ± 0.1 eV.[7] For the La + O(^{3}P) reaction, the corresponding MPKE and HKEO values are 0.67 ± 0.06 and 1.8 ± 0.1 eV. At the time of the original experimental work,[6,7] it was thought, on the basis of available thermochemical values, that the reaction La + O_2 → LaO_2^+ + e^- was exothermic for both $O_2(X^3\Sigma_g)$ and $O_2(a^1\Delta_g)$. However, on the basis of the results of the present work, it is now established that this reaction is endothermic for both $O_2(X^3\Sigma_g)$ and $O_2(a^1\Delta_g)$ (see Table 1). It is clear, therefore, that the reaction La + O_2 → LaO_2^+ + e^- cannot be associated with the chemielectron band observed under the La + $O_2(X^3\Sigma_g)$ reaction conditions. Inspection of Table 1, however, shows that reactions 5 and 6 are both highly exothermic and, likely to be very rapid. This indicates that the chemielectron band observed under the La + $O_2(X^3\Sigma_g)$ reaction conditions arises from

$$La + O_2(X^3\Sigma_g) \rightarrow LaO + O \qquad (5)$$

followed by

$$La + O \rightarrow LaO^+ + e^- \qquad (6)$$

(The equation numbering follows that in Table 1).

Therefore, the chemielectron band observed under the La + $O_2(X^3\Sigma_g)$ reaction conditions should be the same as that observed from the La + O(^{3}P) reaction. Experimentally, these bands certainly have the same shape[7] and, taking into account experimental errors in the MPKE and HKEO values, these bands are very close to each other and can be considered to be the same. The experimental values recorded for the La + $O_2(X^3\Sigma_g)$ reaction (i.e., MPKE = 1.03 ± 0.20 eV, HKEO = 1.50 ± 0.1 eV) are probably the more reliable for reaction 6 as the signal-to-noise in these spectra is better than in those recorded for La + O(^{3}P). The HKEO value expected on the basis of the calculations performed in this work, the negative of the reaction enthalpy of reaction 6, is 2.48 eV. This is greater than the experimental HKEO value of 1.5 ± 0.1 eV probably because of poor Franck−Condon factors in the region of the chemielectron onset. This interpretation means that the LaO^+ observed in the chemion spectrum from the La + O(^{3}P) and La + $O_2(X^3\Sigma_g)$ reaction conditions arises from reaction 6 but that the LaO_2^+ seen in these chemion spectra[7] must arise from ion−molecule reactions such as reaction 11, M + LaO^+ + O → LaO_2^+ + M, or reaction 7, LaO^+ + O_2 → LaO_2^+ + O, which occur in the ion extraction region of the mass spectrometer.

For the La + $O_2(a^1\Delta_g)$ reaction, a very much more intense chemielectron band is observed at higher electron kinetic energy than is observed under the other two reaction conditions. It has a MPKE value of 2.41 ± 0.06 eV and a HKEO value of 3.3 ± 0.1 eV. This is clearly different in position and shape from the La + O(^{3}P) → LaO^+ + e^- chemielectron band. However, assignment of this band is difficult as La + O_2 → LaO_2^+ + e^- is endothermic for $O_2(a^1\Delta_g)$ (see Table 1). The only possible explanation that would be consistent with the experimental results and the reaction enthalpies shown in Table 1 is that reaction 5

$$La + O_2(a^1\Delta_g) \rightarrow LaO + O \qquad \Delta H = -3.37 \text{ eV} \qquad (5)$$

is again followed by

$$La + O \rightarrow LaO^+ + e^- \qquad (6)$$

but that some of the reaction exoergicity of reaction 5 is stored in the oxygen atoms produced (e.g., as O(^{1}D) as this is known to be long-lived with respect to the ground state) and this then undergoes chemiionization via reaction 6 to give chemielectrons with higher kinetic energy than those obtained via La + O(^{3}P) in reaction 6. Reaction 6 with O(^{3}P) has a reaction enthalpy of −2.48 eV and for O(^{1}D) the reaction enthalpy of reaction 6 is −4.45 eV, taking the O(^{1}D) − O(^{3}P) separation as 1.97 eV.[35] The HKEO value of 3.3 ± 0.1 eV, recorded for La + $O_2(a^1\Delta_g)$ reaction conditions, is lower than the negative of the calculated reaction enthalpy of reaction 6, with O(^{1}D) of 4.45 eV, again because of poor Franck−Condon factors in the region of the chemielectron onset.

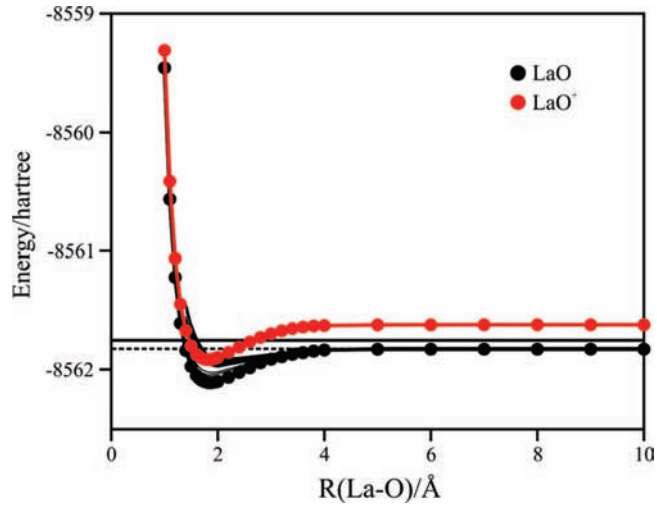

Figure 1. Spin-free potential-energy curves for the ground states of LaO and LaO^+ as well as a number of excited states of LaO. The dotted and solid horizontal lines correspond to La + O(^{3}P) and La + O(^{1}D) calculated dissociation limits, respectively.

Potential Curves for LaO, LaO* and LaO^+. After it was discovered that, for both La + O and La + O_2 reactions, chemiionization arises from La + O → LaO^+ + e^-, a number of excited states of LaO were investigated to understand the chemiionization mechanisms. The electronic states of LaO are of the Σ, Π, Δ, and Φ types. In C_2 symmetry, Σ and Δ states transform as the A irreducible representation, whereas Π and Φ states transform as the B irreducible representation. Doublets and quartets have been considered for LaO, and singlets and triplets have been considered for LaO^+. For LaO, 10 doublets and 10 quartets were computed in each irreducible representation and were included in the spin−orbit calculations. So many states had to be included because of the need to describe the chemiionization region occurring at ca. 8 eV above the ground state. The potential energy curves were calculated at the CASPT2 level of theory and are shown in Figure 1. An enlarged region of this figure of particular interest is given in Figure 2. It is the region where the chemiionization occurs, i.e., the region where the horizontal lines from the La and O(^{3}P) reagents and the La and O(^{1}D) reagents cross excited states of LaO. However, from spin conservation, reaction between La(^{2}D) + O(^{1}D) can only give doublet LaO* excited states, whereas La(^{2}D) and O(^{3}P) can give rise to doublet and quartet LaO* states. The autoionization process LaO* → $LaO^+(^1\Sigma)$ + e^- is a spin-allowed process if ΔS between the initial (LaO excited state) and final (ion plus electron) states is zero. Moreover, the $\Delta\Omega = 0$ selection rule has to be fulfilled between the initial and the final state.

For the La + O(^{1}D) chemiionization reaction, inspection of Figure 2 shows that the reactants approach each other until the horizontal line from the reactants encounters doublet excited states at ca. 1.60 Å. For those states, the $\Delta S = 0$ selection rule for autoionisation is satisfied. As for the $\Delta\Omega = 0$ selection rule, excited states with an Ω value equal to 0.5 will chemiionize to

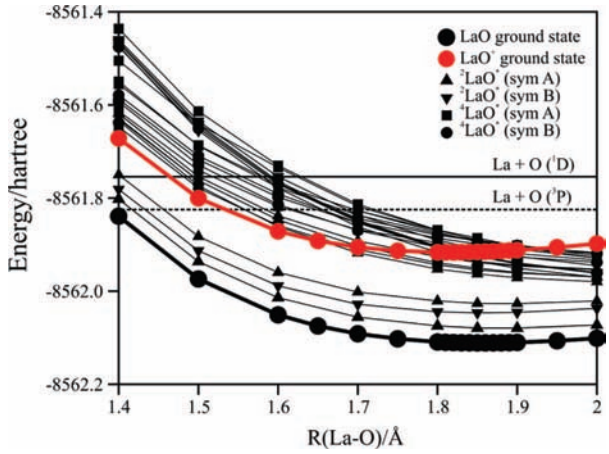

Figure 2. Enlarged region of the spin-free potential-energy curves for a number of excited states of LaO and the ground state of LaO^+ in the region where the chemiionization reactions occur. The dotted and solid horizontal lines correspond to La + O(^{3}P) and La + O(^{1}D) calculated dissociation limits, respectively.

$LaO^+(^1\Sigma) + e^-$. The solid horizontal La + O(^{1}D) line crosses such an LaO* ($^2\Pi_{0.5}$) state at 1.59 Å and at this distance, the LaO* state is located ca. 2.9 eV vertically above the LaO^+ ground state. Thus, the computed chemielectron band maximum is 2.9 eV, which is in a reasonably good agreement with the experimental band maximum of (2.41 ± 0.06 eV).

For La + O(^{3}P), the horizontal (dotted) line from the reactants crosses LaO* states at internuclear distances at ca. 1.7 Å. These are quartet states of LaO and the first one for which the $\Delta\Omega = 0$ rule is fulfilled is a $^4\Delta_{0.5}$ state at 1.72 Å located ca. 2.2 eV vertically above the LaO^+ ground state. However, in the chemiionization process La + O → LaO* → $LaO^+(^1\Sigma) + e^-$, the second step, the autoionization process $LaO^*(^4\Delta) \rightarrow LaO^+(^1\Sigma) + e^-$, is spin-forbidden as the $\Delta S = 0$ selection rule is not satisfied. Therefore, this process is likely to be less intense than a spin-allowed one. The first LaO* state ($^2\Pi_{0.5}$) that fulfills both selection rules is encountered at ca. 1.67 Å and is located 1.9 eV above the LaO^+ ground state. The expected chemielectron band maximum of 1.9 eV is clearly higher that the experimental value of 1.03 ± 0.20 eV. A possible explanation for the rather poor agreement between experimental and theoretical values of the chemielectron band maxima for both La(^{2}D) + O(^{3}P) and La(^{2}D) + O(^{1}D) reactions can be that chemiionization occurs via a series of channels, and what is observed experimentally is a convolution of all these processes. Nevertheless, the expected chemielectron band maximum for La(^{2}D) + O(^{1}D) → $LaO^+ + e^-$ is higher than that for La(^{2}D) + O(^{3}P) → $LaO^+ + e^-$, in agreement with the experimental observations.

For La(^{2}D) + $O_2(X^3\Sigma_g)$ → $LaO(X^2\Sigma)$ + O, it appears from Table 1 that this reaction is sufficiently exothermic to produce O(^{3}P) and O(^{1}D) but that O(^{3}P) is the dominant product. Chemiionization occurs via La(^{2}D) + O(^{3}P) → $LaO^+(X^1\Sigma) + e^-$ to give a chemielectron band with a MPKE value of 1.03 ± 0.20 eV. In contrast, La(^{2}D) + $O_2(a^1\Delta_g)$ → $LaO(X^2\Sigma)$ + O, which is more exothermic, produces a significant amount of O(^{1}D) as evidenced by the production of the higher energy chemielectron band from La(^{2}D) + O(^{1}D) → $LaO^+(X^1\Sigma) + e^-$, with a MPKE value of 2.41 ± 0.06 eV.

4. Conclusions

The chemiionization reactions that occur for the La + O(^{3}P), La + $O_2(X^3\Sigma_g)$, and La + $O_2(a^1\Delta_g)$ reaction conditions have been elucidated by quantum chemical methods. The La + O(^{3}P) case is the simplest to interpret. Chemiionization occurs via reaction 6, La + O → $LaO^+ + e^-$. As was found for the U + O_2 reaction,[9] chemiionization for La + $O_2(X^3\Sigma_g)$ occurs via a two-step process, a rapid first step La + O_2 → LaO + O(^{3}P) (reaction 5) followed by La + O(^{3}P) → $LaO^+ + e^-$ (reaction 6). For La + $O_2(a^1\Delta_g)$, chemiionization occurs via the same two step mechanism. In this case, the experimental chemielectron spectra provide evidence for production of O(^{1}D) from reaction 5 and formation of chemielectrons via La + O(^{1}D) → $LaO^+ + e^-$. For all reaction conditions studied, production of LaO^+, observed in the chemiion mass spectra, is attributed to the primary chemiionization reaction, reaction 6. The LaO_2^+ that is observed in the mass spectra does not arise from a chemiionization reaction; it arises from ion−molecule reactions involving LaO^+.

Accurate potential energy curves have been computed for the ground states of LaO and LaO^+, and a number of excited states of LaO to determine the mechanisms of the La + O(^{3}P) and La + O(^{1}D) chemiionization reactions that give LaO^+ and electrons. Calculated chemielectron band maxima and high kinetic energy offsets for the La + O → $LaO^+ + e^-$ reactions considered provide strong support for the chemiionization mechanisms proposed.

Acknowledgment. This work was supported by the Swiss National Science Foundation (grant nos. 200021-111645/1 and 200020-120007). J.M.D. thanks NERC (UK) for support.

References and Notes

(1) Dyke, J. M.; Shaw, A. M.; Wright, T. G. *J. Phys. Chem.* **1994**, *98*, 6327.
(2) Dyke, J. M. *J. Chem. Soc., Faraday Trans. 2* **1987**, *83*, 69.
(3) Dyke, J. M.; Shaw, A. M.; Wright, T. G. *J. Phys. Chem.* **1995**, *99*, 14207.
(4) Dyke, J. M.; Shaw, A. M.; Wright, T. G. in *Gas-Phase Metal Reactions*; Fontijn, A., Ed., Elsevier: Amsterdam, 1992; p 467.
(5) Fontijn, A. *Pure Appl. Chem.* **1974**, *39*, 287.
(6) Cockett, M. C. R.; Nyulaszi, L.; Veszpremi, T.; Wright, T. G.; Dyke, J. M. *J. Electron Spectrosc. Relat. Phenom.* **1991**, *57*, 373.
(7) Cockett, M. C. R.; Dyke, J. M.; Ellis, A. M.; Wright, T. G. *J. Chem. Soc., Faraday Trans.* **1991**, *87*, 19.
(8) Dyke, J. M.; Ellis, A. M.; Feher, M.; Morris, A. *Chem. Phys. Lett.* **1988**, *145*, 159.
(9) Paulovic, J.; Gagliardi, L.; Dyke, J. M.; Hirao, K. *J. Chem. Phys.* **2005**, *122*, 144317.
(10) Paulovic, J.; Gagliardi, L.; Dyke, J. M.; Hirao, K. *J. Chem. Phys.* **2004**, *120*, 9998.
(11) Roos, B. O. In *Advances in Chemical Physics; Ab Initio Methods in Quantum Chemistry-II*; Lawley, K. P., Ed.; John Wiley & Sons Ltd.: Chichester, England, 1987; p 399.
(12) Andersson, K.; Malmqvist, P.-A.; Roos, B. O. *J. Chem. Phys.* **1992**, *96*, 1218.
(13) Douglas, N.; Kroll, N. M. *Ann. Phys.* **1974**, *82*, 89.
(14) Hess, B. *Phys. Rev. A* **1986**, *33*, 3742.
(15) Roos, B. O.; Lindh, R.; Malmqvist, P.-A.; Veryazov, V.; Widmark, P. O. *Chem. Phys. Lett.* **2005**, *409*, 295.
(16) Malmqvist, P.-A. *Int. J. Quantum Chem.* **1986**, *30*, 479.
(17) Malmqvist, P.-A.; Roos, B. O. *Chem. Phys. Lett.* **1989**, *155*, 189.
(18) Brynda, M.; Gagliardi, L.; Widmark, P. O.; Power, P. P.; Roos, B. O. *Angew. Chem., Int. Ed.* **2006**, *45*, 3804.
(19) Roos, B. O.; Borin, A. C.; Gagliardi, L. *Angew. Chem., Int. Ed.* **2007**, *46*, 1469.
(20) Roos, B. O.; Gagliardi, L. *Inorg. Chem.* **2006**, *45*, 803.
(21) La Macchia, G.; Brynda, M.; Gagliardi, L. *Angew. Chem., Int. Ed.* **2006**, *45*, 6210.
(22) Gagliardi, L.; Roos, B. O. *Nature* **2005**, *43*, 3848.
(23) Gagliardi, L.; Pyykko, P.; Roos, B. O. *Phys. Chem. Chem. Phys.* **2005**, *7*, 2415.
(24) Gagliardi, L.; Heaven, M. C.; Krogh, J. W.; Roos, B. O. *J. Am. Chem. Soc.* **2005**, *127*, 86.
(25) Hagberg, D.; Karlstrom, G.; Roos, B. O.; Gagliardi, L. *J. Am. Chem. Soc.* **2005**, *127*, 14250.

(26) Gagliardi, L.; Willetts, A.; Skylaris, C. K.; Handy, N. C.; Spencer, S.; Ioannou, A. G.; Simper, A. M. *J. Am. Chem. Soc.* **1998**, *120*, 11727.
(27) Stephens, P. J.; Devlin, F. J.; Chabalowski, C. F.; Frisch, M. J. *J. Phys. Chem.* **1994**, *98*, 11623.
(28) Karlstrom, G.; Lindh, R.; Malmqvist, P.-A.; Roos, B. O.; Ryde, U.; Veryazov, V.; Widmark, P. O.; Cossi, M.; Schimmelpfennig, B.; Neogrady, P.; Seijo, L. *Comput. Mater. Sci.* **2003**, *28*, 222.
(29) Toerring, T.; Zimmermann, K.; Hoeft, J. *Chem. Phys. Lett.* **1988**, *151*, 520.
(30) Schroeder, D.; Schwarz, H.; Harvey, J. N. *J. Phys. Chem. A* **2000**, *104*, 11257.
(31) Andrews, L.; Zhou, M.; Chertihin, G. V.; Bauschlicher, C. W. *J. Phys. Chem. A* **1999**, *103*, 6525.
(32) Martin, W. C.; Zalubas, R.; Hagan, L. *Atomic Energy Levels — The Rare Earth Elements*; NSRDS-NBS 60; National Bureau of Standards: Washington, DC, 1978.
(33) (a) Murad, E. *Chem. Phys. Lett.* **1978**, *59*, 359. (b) Murad, E. USAF Report AFGL-TR-0235 Hanscom AFB, MA1977.
(34) Clemmer, D. E.; Dalleska, N. F.; Armentrout, P. B. *Chem. Phys. Lett.* **1992**, *190*, 259.
(35) Moore, C. E. *Atomic Energy Levels*; NBS No. 467; US GPO: Washington, DC, 1949; Vol. 1.
(36) Cao, X.; Dolg, M. *J. Mol. Struct. (THEOCHEM)* **2002**, *581*, 139.
(37) Cao, X.; Dolg, M. *J. Chem. Phys.* **2001**, *115*, 7348.
(38) Küchle, W.; Dolg, M.; Stoll, H. *J. Phys. Chem. A* **1997**, *101*, 7128.
(39) Wu, Z. J.; Guan, W.; Meng, J.; Su, Z. M. *J. Cluster Sci.* **2007**, *18*, 444.
(40) Wang, S. G.; Schwarz, W. H. E. *J. Phys. Chem.* **1995**, *99*, 11687.
(41) Dolg, M.; Stoll, H. In *Handbook on the Physics and Chemistry of Rare Earths*; Gschneidner, K. A., Eyring, L., Eds.; Elsevier: Amsterdam, 1996; Vol. 22.
(42) Huber, K. P.; Herzberg, G. *Molecular Spectra and Molecular Structure, IV, Constants of Diatomic Molecules*; Van Nostrand Reinhold: New York, 1979.
(43) Schofield, K. *J. Phys. Chem. A* **2006**, *110*, 6938.
(44) Cockett, M. C. R.; Dyke, J. M.; Ellis, A. M.; Feher, M.; Wright, T. G. *J. Electron Spectrosc.* **1990**, *51*, 529.

JP804578D